

1 *Supporting Information*

2  
3 Measurement report: Simultaneous measurement on  
4 atmospheric gas- and aerosol-phase water-soluble organics  
5 in Shanghai: Remarkable increase in light absorbing of  
6 Asian dust aerosols during long-range transport  
7

8 Zheng Li<sup>1</sup>, Gehui Wang<sup>1,2\*</sup>, Binyu Xiao<sup>1</sup>, Rongjie Li<sup>1</sup>, Can Wu<sup>1,2\*</sup>, Shaojun Lv<sup>1</sup>, Feng  
9 Wu<sup>3</sup>, Qingyan Fu<sup>4</sup>, Yusen Duan<sup>5</sup>

10  
11 <sup>1</sup>Key Lab of Geographic Information Science of the Ministry of Education, School of  
12 Geographic Sciences, East China Normal University, Shanghai 210062, China

13 <sup>2</sup>Institute of Eco-Chongming, 20 Cuiniao Rd., Chongming, Shanghai 202150, China

14 <sup>3</sup>State Key Laboratory of Loess and Quaternary Geology, Institute of Earth  
15 Environment, Chinese Academy of Science, Xi'an 710061, China

16 <sup>4</sup>Key Laboratory of Formation and Prevention of Urban Air Pollution Complex, Ministry  
17 of Ecology and Environment, Shanghai Academy of Environmental Sciences, Shanghai,  
18 200233, China

19 <sup>5</sup>Shanghai Technology Center for Reduction of Pollution and Carbon Emissions,  
20 Shanghai, 200233, China

21  
22  
23  
24 Correspondence to: Prof. Gehui Wang ([ghwang@geo.ecnu.edu.cn](mailto:ghwang@geo.ecnu.edu.cn)) and Dr. Can Wu  
25 ([cwu@geo.ecnu.edu.cn](mailto:cwu@geo.ecnu.edu.cn))  
26  
27  
28  
29  
30

31 This PDF file includes:

32 1. Four texts, Text S1-S4

33 2. One table, Table S1

34 3. Five figures, Figure S1-S5

35 4. References  
36

### 37 **Text S1 Detailed description of the instruments**

38 The ambient air was sampled and separated by a PM<sub>2.5</sub> sharp cut cyclone with a  
39 flow rate of 16.7 L/min. Then, the air was drawn through the passageway between the  
40 inner and outer Pyrex glass tubes in wet annular denuder (WAD) system. In WAD  
41 system, gaseous samples were wetted with pure water and collected. Scrub and Impact  
42 Aerosol Collector (SCI) was placed downstream of the WAD for collecting aerosol  
43 phase samples. The gas and aerosol samples were subsequently injected into the ion  
44 chromatography (ICS-5000+, Thermo Scientific) for analysis of water-soluble inorganic  
45 ions and small molecular organic acids after removing the insoluble species and bubbles.

46 The gas and particle-phase water-soluble organic carbon and water-soluble organic  
47 nitrogen (WSOC/WSON) were simultaneous determined by using a TOC/TN analyzer  
48 (TOC-L CPH, Shimadzu, Japan). The concentrations of WSOC were calculated as the  
49 difference between water-soluble total carbon (WSTC) and water-soluble inorganic  
50 carbon (WSIC). Similar, the concentrations of WSON were calculated as the difference  
51 between water-soluble total nitrogen (WSTN) and water-soluble inorganic nitrogen  
52 (WSIN).

53 Organic carbon (OC) and elemental carbon (EC) were determined by DRI Model  
54 2015 Carbon Analyzer (Atmoslytic, Inc., Calabasas, USA) with IMPROVE\_A protocol  
55 (Chow et al., 2007).

### 56 **Text S2 Measurement of organic aerosol in filter samples**

57 Organic compounds including nitroaromatic compounds (NACs) were analyzed by  
58 using gas chromatography mass spectroscopy (GC/MS, Agilent Co.). One quarter of  
59 filter was extracted with the mixture of methanol and dichloromethane (v:v, 1:2). After  
60 ultrasonic extraction, the extracts were concentrated to dryness and reacted with 50  $\mu$ L

61 N,O-bis-(trimethylsilyl)trifluoroacetamide (BSTFA) with 1% trimethylsilyl and 10  $\mu$ L of  
62 pyridine at 70  $^{\circ}$ C for 3 h. Then, the extracts were analyzed by GC/MS. The detected  
63 compounds recoveries were better than 85%. In this study, only four NACs were  
64 determined, which are 4-nitrophenol (4NP), 2-methoxy-4-nitrophenol (4NGA), 2-  
65 methoxy-5-nitrophenol (5NGA), and 5-nitrosalicylic acid (5NSA).

66 One quarter of filter was used to analyze imidazoles (IMs). More information about  
67 this analysis method can be found in our previous study (Liu et al., 2023). Herein, total  
68 of eight IMs were determined, including 2-methylimidazole, 4(5)-methylimidazole, 1-  
69 ethylimidazole, 2-ethylimidazole, 1-phenylimidazole, 2-phenylimidazole, 2-  
70 imidazolcarboxaldehyde and 4-imidazolcarboxaldehyde. The details of the analytical  
71 method can be found in our previous studies (Wang et al., 2006; Liu et al., 2023; Liu et  
72 al., 2024).

### 73 **Text S3 Absorption spectra of water-soluble BrC analysis**

74 The light absorption spectra of the water-soluble BrC was measured by a UV-vis  
75 spectrometer (T6 New Century, Persee) over a wavelength range of 200 – 900 nm (Wu  
76 et al., 2024). The light absorption coefficients ( $Abs_{\lambda}$ ,  $M m^{-1}$ ) of the water extracts was  
77 calculated by eq (1).

$$78 \quad Abs_{\lambda} = (A_{\lambda} - A_{700}) \frac{V_l}{V_a \times l} \times \ln(10) \quad (1)$$

79 where  $A_{\lambda}$  and  $A_{700}$  represent the light absorption at the wavelengths of  $\lambda$  and 700 nm  
80 measured by the UV-vis spectrometer.  $V_l$  refers to the volume of solvent extract.  $V_a$  refers  
81 to the sampling volume and  $l$  corresponds to the path length of the cell (1 cm).

82 The mass absorption coefficient ( $MAC_{\lambda}$ ,  $m^2 g^{-1}$ ) of the extracts at the wavelength of  
83  $\lambda$  can be quantified as eq (2)

$$84 \quad MAC_{\lambda} = \frac{Abs_{\lambda}}{M} \quad (2)$$

85 where M represent the concentration of WSOC.

86 **Text S4 Contribution of organic matter to aerosol liquid water content (ALWC)**

87 Here we used the ALWC calculation method reported by Lv et al (2022b; 2022a).

88 The contribution of organic matter (OM) to ALWC ( $ALWC_{org}$ ) were defined as the

89 following eq (3)

90 
$$ALWC_{org} = \frac{[OM]\rho_w}{\rho_{org}} \frac{\kappa_{org}}{\frac{1}{RH}-1} \quad (3)$$

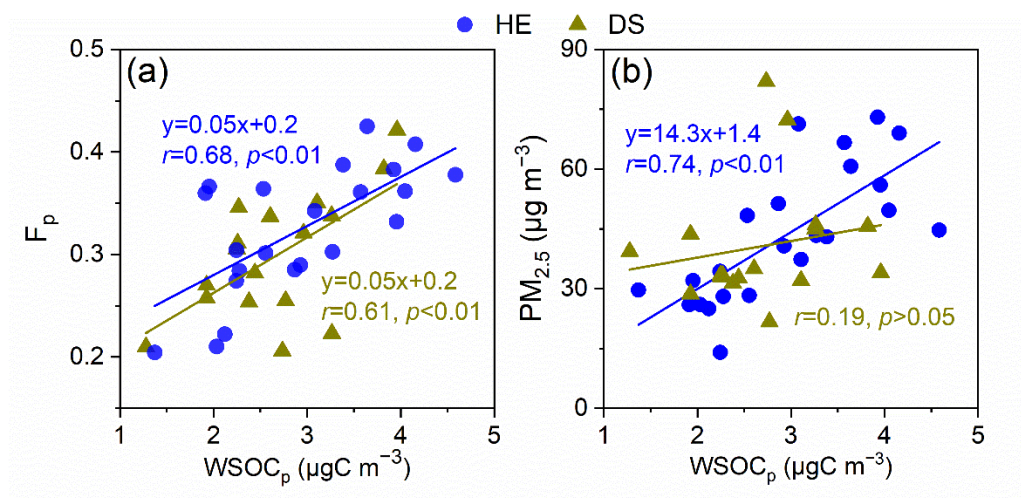
91 where OM is the mass concentration of organics,  $\rho_w$  is the density of water,  $\rho_{org}$  is the

92 density of OM ( $1.4 \text{ g cm}^{-3}$ ).  $\kappa_{org}$  is the hygroscopicity parameter of OM (0.06).

93 **Table S1.** Relative abundances (%) of ammonium, nitrate, and sulfate in PM<sub>2.5</sub> or PM<sub>10</sub>  
 94 during dust storm periods in different regions of China.

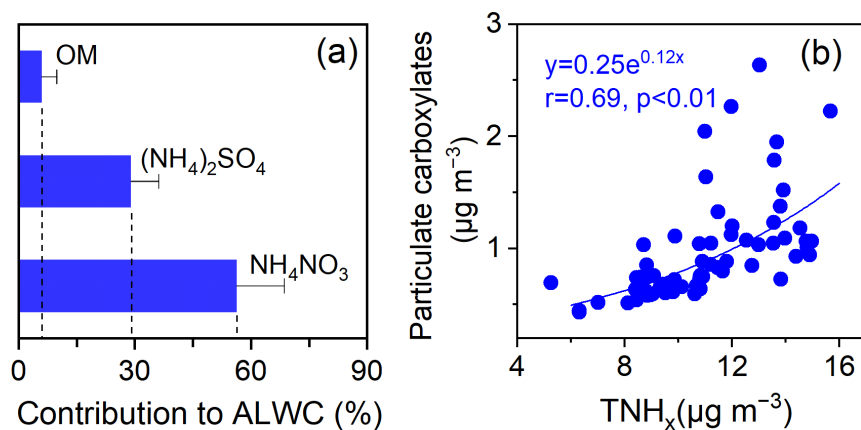
Sampling site		Sampling time	NH <sub>4</sub> <sup>+</sup>	NO <sub>3</sub> <sup>-</sup>	SO <sub>4</sub> <sup>2-</sup>	Type	Reference
Desert region	Tengger	03, 2023	0.03	0.5	4.1	PM <sub>10</sub>	This study
	Taklimakan	04, 2008	-	0.3	4.2	PM <sub>2.5</sub>	(Wu et al., 2012)
Upwind region	Tongyu	04-06, 2006	0.18	1.26	2.43	PM <sub>2.5</sub>	(Shen et al., 2011)
	Yulin	2006-2008	0.45	0.81	3.53	PM <sub>2.5</sub>	(Wang et al., 2011)
Downwind region	Shanghai	10, 2019	3.8	10.1	6.4	PM <sub>2.5</sub>	(Wu et al., 2020)
	Shanghai	03-04, 2023	3.3	8.1	5.3	PM <sub>2.5</sub>	This study

95  
 96  
 97  
 98  
 99  
 100  
 101  
 102



103  
 104 **Figure S1.** Linear regression analysis for WSOC<sub>p</sub> with (a) partitioning coefficient of  
 105 WSOCs (F<sub>p</sub>) and (b) PM<sub>2.5</sub> during the haze event (HE) and dust storm (DS) event,  
 106 respectively

107  
 108  
 109



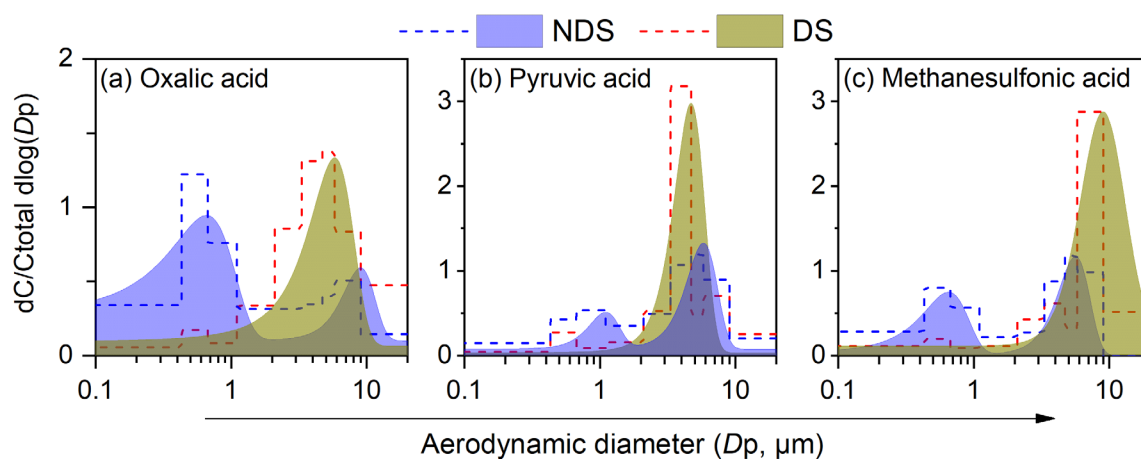
110

111 **Figure S2.** (a) Contributions of  $\text{NH}_4\text{NO}_3$ ,  $(\text{NH}_4)_2\text{SO}_4$  and OM to ALWC in the haze  
 112 event (HE); (b) Particulate carboxylates as a function of  $\text{TNH}_x$  in the haze event (HE).

113

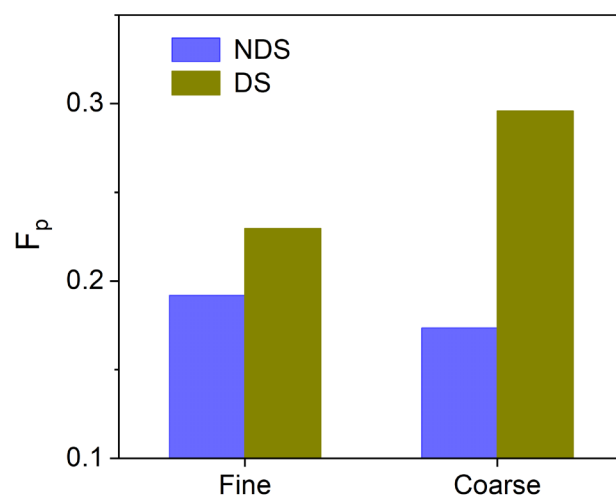
114

115



1

117 **Figure S3.** Size distribution of (a) oxalic acid, (b) pyruvic acid and (c) methanesulfonic  
 118 acid during the non-dust storm (NDS) and dust storm (DS) events in Shanghai.



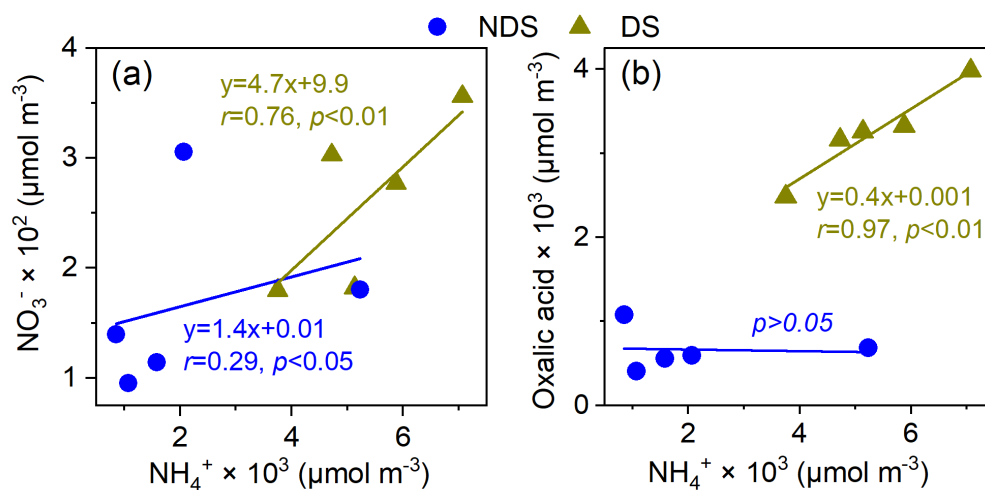
119

120 **Figure S4.** The partitioning coefficients ( $F_p$ ) of WSOCs in the fine (<math><2.1\mu\text{m}</math>) and coarse  
 121 (>math>>2.1\mu\text{m}</math>) in the non-dust storm (NDS) and dust storm (DS) periods in Shanghai during  
 122 spring of 2023.

123

124

125



126

127 **Figure S5.** Linear fit regression for the  $\text{NH}_4^+$  with (a)  $\text{NO}_3^-$  and (b) oxalic acid in coarse  
 128 mode (>math>>2.1\mu\text{m}</math>) of particles in the non-dust storm (NDS) and dust storm (DS) periods in  
 129 Shanghai during spring of 2023.

130

131 **References**

- 132 Chow, J. C., Watson, J. G., Chen, L. W. A., Chang, M. C. O., Robinson, N. F., Trimble, D., and  
133 Kohl, S.: The IMPROVE\_A Temperature Protocol for Thermal/Optical Carbon Analysis:  
134 Maintaining Consistency with a Long-Term Database, *J Air Waste Manage*, 57, 1014-1023,  
135 10.3155/1047-3289.57.9.1014, 2007.
- 136 Liu, X., Wang, H., Wang, F., Lv, S., Wu, C., Zhao, Y., Zhang, S., Liu, S., Xu, X., Lei, Y., and Wang,  
137 G.: Secondary Formation of Atmospheric Brown Carbon in China Haze: Implication for an  
138 Enhancing Role of Ammonia, *Environ Sci Technol*, 57, 11163-11172,  
139 10.1021/acs.est.3c03948, 2023.
- 140 Liu, X., Wu, C., Li, Z., Li, R., Wang, F., Lv, S., Li, R., Zhang, F., Wang, H., Liang, C., Zhang, L.,  
141 and Wang, G.: Atmospheric brown carbon in China haze is dominated by secondary  
142 formation, *Sci Total Environ*, 945, 173901, <https://doi.org/10.1016/j.scitotenv.2024.173901>,  
143 2024.
- 144 Lv, S. J., Wu, C., Wang, F. L., Liu, X. D., Zhang, S., Chen, Y. B., Zhang, F., Yang, Y., Wang, H.  
145 L., Huang, C., Fu, Q. Y., Duan, Y. S., and Wang, G. H.: Nitrate-Enhanced Gas-to-Particle-  
146 Phase Partitioning of Water- Soluble Organic Compounds in Chinese Urban Atmosphere:  
147 Implications for Secondary Organic Aerosol Formation, *Environ Sci Tech Lett*,  
148 10.1021/acs.estlett.2c00894, 2022a.
- 149 Lv, S. J., Wang, F. L., Wu, C., Chen, Y. B., Liu, S. J., Zhang, S., Li, D. P., Du, W., Zhang, F., Wang,  
150 H. L., Huang, C., Fu, Q. Y., Duan, Y. S., and Wang, G. H.: Gas-to-Aerosol Phase Partitioning  
151 of Atmospheric Water-Soluble Organic Compounds at a Rural Site in China: An Enhancing  
152 Effect of NH<sub>3</sub> on SOA Formation, *Environ Sci Technol*, 56, 3915-3924,  
153 10.1021/acs.est.1c06855, 2022b.
- 154 Shen, Z., Wang, X., Zhang, R., Ho, K., Cao, J., and Zhang, M.: Chemical Composition of Water-  
155 soluble Ions and Carbonate Estimation in Spring Aerosol at a Semi-arid Site of Tongyu, China,  
156 *Aerosol Air Qual Res*, 11, 360-368, 10.4209/aaqr.2011.02.0010, 2011.
- 157 Wang, G. H., Kawamura, K., Lee, S., Ho, K. F., and Cao, J. J.: Molecular, seasonal, and spatial  
158 distributions of organic aerosols from fourteen Chinese cities, *Environ Sci Technol*, 40, 4619-  
159 4625, 10.1021/es060291x, 2006.
- 160 Wang, Q., Zhuang, G., Li, J., Huang, K., Zhang, R., Jiang, Y., Lin, Y., and Fu, J. S.: Mixing of dust  
161 with pollution on the transport path of Asian dust — Revealed from the aerosol over Yulin,  
162 the north edge of Loess Plateau, *Sci Total Environ*, 409, 573-581,  
163 <https://doi.org/10.1016/j.scitotenv.2010.10.032>, 2011.
- 164 Wu, C., Liu, X., Zhang, K., Zhang, S., Cao, C., Li, J., Li, R., Zhang, F., and Wang, G.:  
165 Measurement report: Formation of tropospheric brown carbon in a lifting air mass, *Atmos.*  
166 *Chem. Phys.*, 24, 9263-9275, 10.5194/acp-24-9263-2024, 2024.



167 Wu, C., Zhang, S., Wang, G. H., Lv, S. J., Li, D. P., Liu, L., Li, J. J., Liu, S. J., Du, W., Meng, J.  
168 J., Qiao, L. P., Zhou, M., Huang, C., and Wang, H. L.: Efficient Heterogeneous Formation of  
169 Ammonium Nitrate on the Saline Mineral Particle Surface in the Atmosphere of East Asia  
170 during Dust Storm Periods, *Environ Sci Technol*, 54, 15622-15630, 10.1021/acs.est.0c04544,  
171 2020.

172 Wu, F., Zhang, D., Cao, J., Xu, H., and An, Z.: Soil-derived sulfate in atmospheric dust particles  
173 at Taklimakan desert, *Geophysical Research Letters*, 39,  
174 <https://doi.org/10.1029/2012GL054406>, 2012.

175